

# Magnetic properties of epitaxial $\text{YBa}_2\text{Cu}_3\text{O}_x$ films

A. A. Zhukov, V. V. Moshchalkov, V. D. Kuznetsov,<sup>1)</sup> V. V. Metlushko, G. T. Karapetrov, E. V. Pechen,<sup>2)</sup> and I. V. Timashev<sup>1)</sup>

*M. V. Lomonosov State University, Moscow*

(Submitted 18 February 1991)

Zh. Eksp. Teor. Fiz. **100**, 605–624 (August 1991)

It is shown that the  $P_m(B, T)$  magnetization curves of epitaxial  $\text{YBa}_2\text{Cu}_3\text{O}_x$  films can be described by a universal scaling law over a wide temperature range (20–80 K). The temperature and field dependence of the critical current density is studied. The field dependence of the thermally activated magnetic flux creep is investigated. The activation energy of Abrikosov vortices is determined to be 0.25 eV at  $T = 70$  K.

## INTRODUCTION

The study of thin films of HT-SC's is now receiving close attention throughout the world. This interest is mainly aroused by the possibility of applying HT-SC films in microelectronics.<sup>1</sup> In addition, these films even exceed single-crystal HT-SC's in a number of parameters, for example the critical current density  $j_c$  for good films at liquid nitrogen temperature is  $\geq 10^6$  A/cm<sup>2</sup>, which is an order of magnitude greater than in single crystals. However, the reason for the difference in superconducting parameters between films and single-crystal specimens is, as yet, unexplained. In this connection we have undertaken a comprehensive study of the magnetic properties—the Meissner effect, magnetic flux creep, the temperature and field dependences of critical current—in thin  $\text{YBa}_2\text{Cu}_3\text{O}_x$  films.

## METHOD

Specimens for the investigation were prepared from single-crystal epitaxial  $\text{YBa}_2\text{Cu}_3\text{O}_x$  films, obtained by magnetron sputtering of a stoichiometric target with deposition onto a single-crystal  $\text{SrTiO}_3$  (100) substrate heated to 680–850 °C without subsequent annealing.<sup>2</sup>

A series of specimens was prepared: two 1.9 mm diameter disks and two thin rings with outer diameter 1.9 mm and inner diameter 1.5 mm. The film thickness was 3500 Å, the superconducting transition temperature  $T_c \approx 90.5$  K. The specimens were cut from the film together with the substrate, using a cylindrical copper bit holding a diamond suspension in turpentine.

Measurement of the magnetic properties was carried out with a SQUID<sup>3</sup> and a vibrational (PAR-155) magnetometer. For measurements with the SQUID magnetometer the specimens were stuck with Apiezon grease to the bottom of a quartz container which was evacuated, sealed off, and filled with spectroscopically pure helium at a pressure  $\sim 20$  torr. For measurements with the vibration magnetometer the specimens were stuck to a holder with “Ramsay” vacuum grease.

## EXPERIMENTAL RESULTS

### Field and temperature dependence of the magnetic moment

The initial sections of the plots of the magnetic moment  $P_m$  versus the external magnetic field  $B$  at different temperatures are shown in Fig. 1. The curves were obtained by cooling the specimens in zero field ( $< 10^{-5}$  T) with subsequent application of the field and correspond to the zero field cool-

ing (ZFC) regime. As can be seen from Fig. 1, the value of the lower critical field  $B_{c1}$  with the field oriented perpendicular to the plane of the disk ( $\mathbf{B} \parallel \mathbf{c}$ ) is anomalously small—the departure from linearity of the  $P_m(B)$  relation starts practically from zero field even at  $T = 4.2$  K. This is explained by the large demagnetizing of the film for which the demagnetizing factor  $N$  is very close to 1 ( $N \approx 1 - \pi h / 2D$ , where  $h$  is the thickness and  $D$  is the diameter of the disk). The same results were obtained earlier<sup>4</sup> for a thin ( $\approx 2600$  Å.) Sn film for the field oriented perpendicular to the plane of the substrate.

Magnetization curves for a  $\text{YBa}_2\text{Cu}_3\text{O}_x$  disk at different temperatures are shown in Fig. 2. The characteristic feature of the  $P_m(B)$  curves, unlike similar curves obtained for single-crystals of  $\text{YBa}_2\text{Cu}_3\text{O}_x$  (Ref. 5) and  $\text{Bi}_2\text{Sr}_2\text{Ca}_1\text{Cu}_2\text{O}_x$  (Ref. 6) is that the maximum  $P_m(B)$  on magnetic reversal is reached near  $B = 0$  and the magnetization curves themselves are close in shape to a rhombus. A similar behavior was observed earlier for films of  $\text{TlBaCaCuO}$  (Ref. 7) and  $\text{BiSrCaCuO}$  (Ref. 8) and it corresponds to the case when the irreversible part of the magnetization  $P_m(B)$  curves determined by pinning is much greater

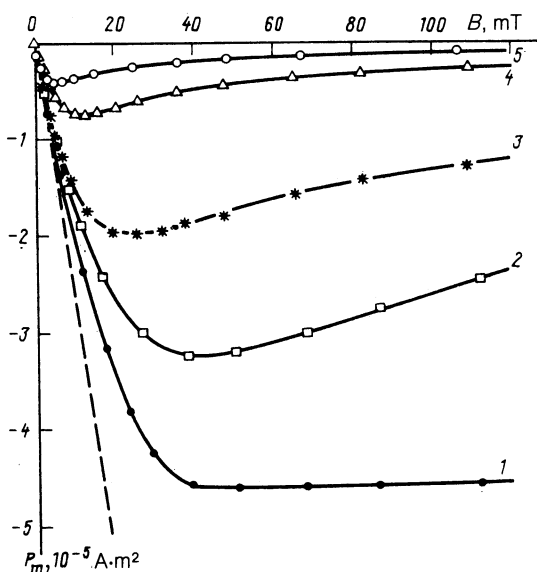


FIG. 1. Initial sections of the field dependence of the magnetic moment of a disk of  $\text{YBa}_2\text{Cu}_3\text{O}_x$  film,  $\mathbf{B} \parallel \mathbf{c}$ , after ZFC: 1)  $T = 4.2$  K; 2) 30 K; 3) 50 K; 4) 70 K; 5) 80 K. The dashed line shows the slope corresponding to ideal diamagnetism  $P_m = -H/(1-N)$ ,  $N$  being the demagnetizing factor of a disk of film.

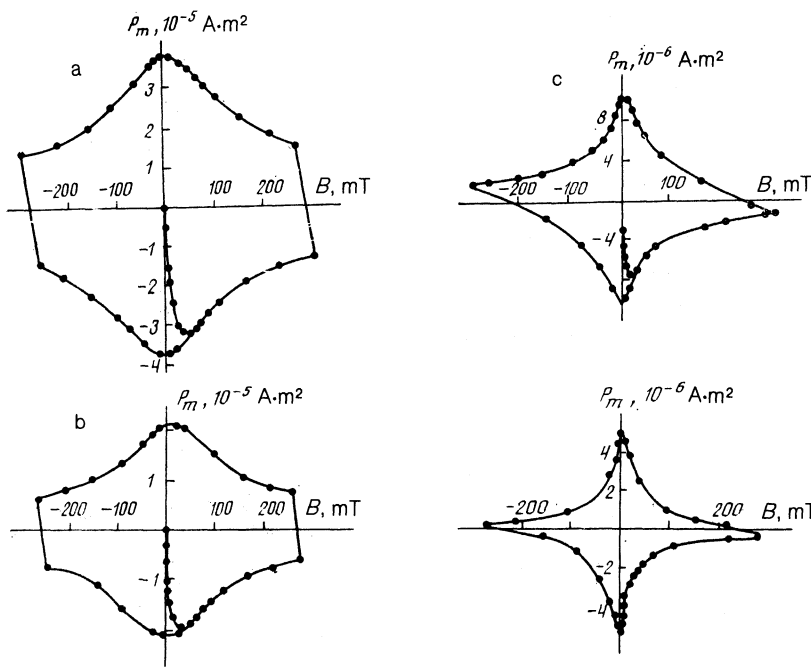


FIG. 2. Field dependence of the magnetic moment  $P_m$  of a disk of  $\text{YBa}_2\text{Cu}_3\text{O}_x$  film,  $\mathbf{B}||\mathbf{c}$ , after ZFC: a)  $T = 30 \text{ K}$ ; b)  $50 \text{ K}$ ; c)  $70 \text{ K}$ ; d)  $80 \text{ K}$ .

than the reversible part of  $P_m(B)$ , associated with magnetization of a vortex lattice.<sup>9</sup>

Analysis of the magnetization curves shows that they have similar shape; over a wide temperature range (20–80 K), as can be seen in Fig. 3, a universal relation holds

$$P_m(B, T) = P_0(T) \varphi_s(B/\mu_0 P_0(T)),$$

where  $P_0(T) = P_m(0, T)$ ,  $\mu_0$  is the permeability of the vacuum,  $\varphi_s$  is the scaling function and  $\varphi_s(0) = \pm 1$ . Such behavior was observed earlier in  $\text{Tl}_2\text{Ba}_2\text{Ca}_2\text{Cu}_3\text{O}_{10}$  ceramics.<sup>10</sup>

The  $P_m^{\text{ZFC}}(T)$  temperature dependence measured in the ZFC regime with subsequent application of the field  $B$  for  $T < T_c$  and heating in the same field has been studied for thin films more than once (see, for example Refs. 6, 7). At the same time the temperature variation of the magnetic moment  $P_m^{\text{FC}}(T)$ , obtained by cooling in a field (FC) has so far not been studied, mainly apparently because of the small value of the response. Hatta *et al.*<sup>7</sup> mentioned only that  $P^{\text{FC}}$

for  $\text{TlBaCaCuO}$  films is much less than  $P_m^{\text{ZFC}}$  and disappears at  $T \approx 70 \text{ K} < T_c$ , unlike  $P_m^{\text{ZFC}}$ .

The  $P_m^{\text{FC}}(T)$  dependence has been obtained in the present work for  $\text{YBa}_2\text{Cu}_3\text{O}_x$  film specimens in the form of disks and rings for different fields  $B$ . Curves of  $P_m^{\text{FC}}(T)$  obtained in fields  $B = 23.63 \text{ mT}$  and  $B = 40.74 \text{ mT}$  are shown in Fig. 4. The  $P_m^{\text{ZFC}}(T)$  dependence is also shown there for  $B = 6.29 \text{ mT}$ . A “paramagnetic” response as well as the expected diamagnetic was found for a disk of  $\text{YBa}_2\text{Cu}_3\text{O}_x$  film in the FC regime. In addition, the magnetic moment  $P_m^{\text{FC}}$  obtained is metastable and its value could change discontinuously when the temperature was subsequently lowered or even for constant external conditions.

All these facts compelled us to analyze in detail the shape of the magnetometer response when the specimen was moved between the pick-up coils of the flux converter. The response curve of the magnetometer to the movement of a disk between the pick-up coils is shown in Fig. 5. The planes of the loops are indicated by the dashed lines. The abscissa

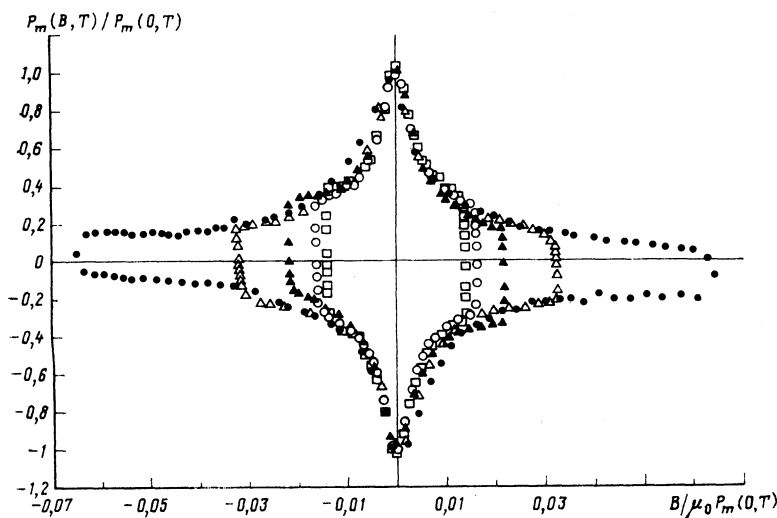


FIG. 3. Dependence of  $P_m(B, T)/P_m(0, T)$  on  $B/\mu_0 P_m(0, T)$  for different temperatures:  $\square$ )  $T = 29 \text{ K}$ ;  $\circ$ )  $38 \text{ K}$ ;  $\blacktriangle$ )  $51.5 \text{ K}$ ;  $\triangle$ )  $65 \text{ K}$ ;  $\bullet$ )  $77 \text{ K}$ .

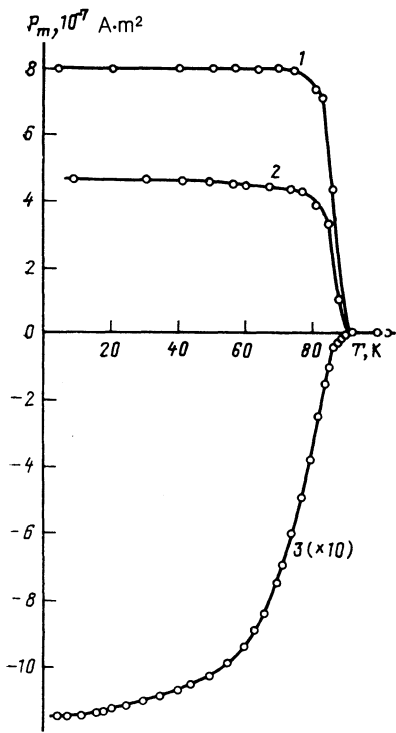


FIG. 4. Temperature dependence of the magnetic moment  $P_m$  of a disk of  $\text{YBa}_2\text{Cu}_3\text{O}_x$  film,  $\mathbf{B} \parallel \mathbf{c}$ : 1)  $B = 23.63$  mT (FC); 2)  $B = 40.74$  mT (FC); 3)  $B = 6.29$  mT (ZFC).

axis corresponds to the position of the specimen on the  $z$  axis of the gradientometer, the magnetometer signal  $\Phi(z)$  is plotted vertically. In this case the feature of the behavior of the signal is the destruction of the symmetry of the signal about the center of the distance between the pick-up coils of the flux converter.

The signal for a point dipole is symmetrical about the center of the distance between the coils and is shown in Fig. 5b. The usual diamagnetic response, obtained on this same disk after ZFC and application of the field, had just this shape. The curve has only two extrema, as it should in the case of a point dipole.<sup>11</sup>

The signal shown in Fig. 5a is strictly speaking neither paramagnetic nor diamagnetic. The "paramagnetic" sign of the signal  $P_m^{\text{FC}}$  in Fig. 4 is connected with the standard measuring procedure adopted, for which the signal is determined by the difference between two successive extrema (shown by arrows in Fig. 5a).

The shape of the  $P_m^{\text{FC}}$  response curves obtained on disks and rings of  $\text{YBa}_2\text{Cu}_3\text{O}_x$  film brings to mind above all the superposition of responses from point magnetic moments,

distributed along the  $z$  axis.<sup>12</sup> The dimension of the film specimens in the vertical direction can be considered almost equal to zero. Moments noticeably spaced along the  $z$  axis can thus not be expected to arise. For our flux converter configuration (radius of pick-up coils  $R = 14$  mm, distance between the coils 28 mm) such a specimen appears a point dipole to an accuracy better than 1% (Ref. 12).

Anticipating the further analysis, we should point out a number of factors important for the discussion below. First of all, the anomalously low value of the signal in the FC regime should be noted (as seen in Fig. 4,  $P_m^{\text{FC}} = 4.6 \times 10^{-7}$  A·m<sup>2</sup> for  $B = 40.74$  mT). The moment for a field of 40.74 mT corresponding to a 100% Meissner effect comes to

$$P_m^{\text{full}} = \frac{VB}{\mu_0(1-N)} \approx \frac{D^3B}{2\mu_0} \approx 1.1 \cdot 10^{-4} \text{ A} \cdot \text{m}^2,$$

where  $V$  is the specimen volume. The value of the signal in the ZFC regime is also fairly large (at  $T = 4.2$  K for  $B = 40.74$  mT  $P_m^{\text{ZFC}} = 4.75 \times 10^{-5}$  A·m<sup>2</sup>). The value of the susceptibility in the FC regime  $\chi^{\text{FC}} = P_m^{\text{FC}}/P_m^{\text{full}}$  is very low for  $\text{YBa}_2\text{Cu}_3\text{O}_x$  films,  $\approx 4 \times 10^{-3}$ . In this case, therefore, the stability of the value and the orientation of the magnetic field are very significant, since the reaction of the specimen to a small change in field gives a value of  $\chi$  close to  $k - 1$ . It is limited in absolute magnitude by the value of  $P_m^{\text{ZFC}}$ . The stability of the magnetic field in our measuring set-up is achieved by a niobium-titanium tube and reaches  $\sim 10^{-5}$  T/day.<sup>3</sup>

Zhukov *et al.*<sup>13</sup> have shown that in superconductors with strong pinning the Meissner effect is of an unusual nature. The ejection of Abrikosov vortices from the specimen is hindered by pinning forces. As a result, shielding currents arise which provide a positive (paramagnetic) moment, compensating the negative magnetization of the vortex lattice. In the absence of pinning, this negative magnetization corresponds to the total Meissner effect. The resulting signal in superconductors with strong pinning is appreciably less and the relative magnitude of the signal falls sharply with field. Demagnetizing effects in films produce an amplification of the applied field. Thus, even fields that are small in magnitude correspond to a very small Meissner effect.

The smallness of the magnetic moment indicates that the density  $n = B/\Phi_0$  of Abrikosov vortices differs little from the equilibrium value  $n_0 = \mu_0 H_i/\Phi_0$ , where  $H_i$  is the applied internal field, taking demagnetization into account, and  $\Phi_0$  is a quantum of magnetic flux. As a result, the fluctuations in the demagnetizing field and pinning parameters, resulting from the actual inhomogeneities which exist, can lead to a situation where  $n_0$  is less than  $n$ , i.e., the local paramagnetic magnetization  $m = B/\mu_0 - H_i = (n - n_0)\Phi_0/$

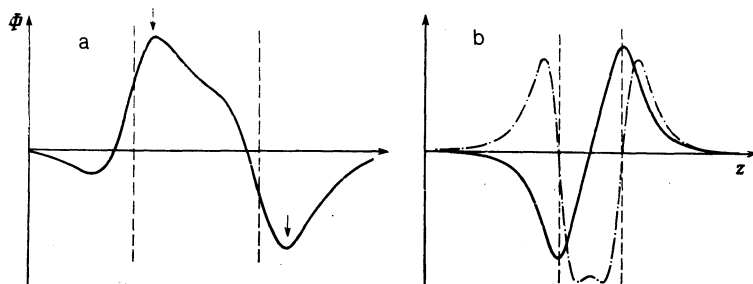


FIG. 5. a) Dependence of SQUID magnetometer response on position of disk of  $\text{YBa}_2\text{Cu}_3\text{O}_x$  film relative to the pick-up loops of the magnetic flux converter (dashed lines) for  $T = 4.2$  K,  $B = 10$  mT,  $\mathbf{B} \parallel \mathbf{c}$ . b) Results of calculation of the magnetometer response on shifting the specimen in the neighborhood of a point dipole (full line) and for two magnetic moments oppositely directed equal in magnitude and displaced along the  $z$  axis (dashed-dot line).

$\mu_0$ . Such a situation was observed experimentally with the help of magnetic decoration near twin boundaries.<sup>14</sup> Macroscopic nonuniform magnetic states of oscillating sign were observed by Leiderer *et al.*<sup>15</sup> on polycrystalline films and ceramic specimens of  $\text{YBa}_2\text{Cu}_3\text{O}_x$ . Yet another factor leading to an increase in vortex density  $n$  is thermal contraction of the specimen. Although the change in  $n$  is then not great, it can be of the same order of magnitude as the small difference  $n - n_0$ .

It should be remarked that in the case of a thin disk the fields produced by the shielding currents at the center and at the edge of the disk have opposite signs,<sup>16,17</sup> and this can also lead to the appearance of a nonuniform state with oppositely magnetized regions.

To explain the shape of the observed magnetometer response, it can be assumed that dia- and paramagnetic regions arise in the film after the superconducting transition. Two opposite moments  $P_m^+$  and  $P_m^-$  can be treated as the simplest model, situated within the boundaries of one and the same specimen. The shape of the response will then be determined by the dependence on the  $z$  coordinate of the specimen of the total magnetic flux  $\Phi$  in loops 1 and 2 of the magnetometer:

$$\begin{aligned} \Phi &= \Phi_1^+ + \Phi_1^- - \Phi_2^+ - \Phi_2^- \\ &= \int_1 \mathbf{A}^+ \cdot d\mathbf{l} + \int_1 \mathbf{A}^- \cdot d\mathbf{l} - \int_2 \mathbf{A}^+ \cdot d\mathbf{l} - \int_2 \mathbf{A}^- \cdot d\mathbf{l}, \end{aligned} \quad (1)$$

where  $d\mathbf{l}$  is an element of the "circumference" of the flux converter coil, and  $\mathbf{A}$  is the vector potential:

$$\mathbf{A} = \frac{\mu_0}{4\pi} \frac{[\mathbf{P}_m \times \mathbf{r}]}{r^3}, \quad (2)$$

where  $\mathbf{r}$  is the radius vector from the magnetic moment to the given point on the circumference. The symbols "−" in front of the magnetic fluxes through the second loop take account of the astatic winding of the flux converter.

With such a model, the experimental dependence of the magnetometer response can be described satisfactorily. As is easily verified, after straightforward integration of Eqs. (1) and (2) for a single point dipole parallel to the axis, the response of the system can be represented by the expression

$$\begin{aligned} \Phi_1(z) = P_m \varphi(z) &= \frac{\mu_0 P_m R^2}{2} \left[ \frac{1}{[R^2 + (l/2 - z)^2]^{3/2}} \right. \\ &\quad \left. - \frac{1}{[R^2 + (l/2 + z)^2]^{3/2}} \right], \end{aligned} \quad (3)$$

where  $z$  is measured along the magnetometer axis relative to the middle of the pick-up coils of the converter, and  $R$  and  $l$  are the radius of a coil and the distance between them, respectively. For two dipoles parallel to the  $z$  axis and separated by a small distance  $\Delta z$ , we have

$$\begin{aligned} \Phi_2(z) &= P_m^+ \varphi_1(z) + P_m^- \varphi_2(z + \Delta z) \\ &\approx (P_m^+ + P_m^-) \varphi(z) + P_m^- (d\varphi/dz) \Delta z, \end{aligned} \quad (4)$$

where

$$\frac{d\varphi}{dz} = \frac{3\mu_0 R^2}{2} \left[ \frac{l/2 - z}{[R^2 + (l/2 - z)^2]^{5/2}} + \frac{l/2 + z}{[R^2 + (l/2 + z)^2]^{5/2}} \right].$$

In general, the second term in Eq. (4) will be apprecia-

bly smaller than the first. However, if  $P_m^+$  and  $P_m^-$  are opposite in sign and close in magnitude,  $|P_m^+| \approx |P_m^-| = P_m$  holds so that we have  $|P_m^+ + P_m^-| = |\Delta P_m| \ll P_m$ , then these two terms can be comparable and for  $\Delta P_m = 0$  only the second term remains. As can be seen from Fig. 5 and Eq. (3),  $\varphi(z)$  and  $d\varphi/dz$  behave differently. If the first is an odd function in  $z$  then  $d\varphi/dz$  is even in  $z$ . It is clear that their total will be asymmetrical about the midpoint between the pick-up coils of the flux converter.

The experimental dependence of the magnetometer response can be described with the help of Eq. (4). In particular, this can be done for the results given in Fig. 5a for  $P_m \Delta z / \Delta P_m R \approx 1.7$ . The value of  $\Delta P_m$  can be calculated from the difference between the signals corresponding to the position of the specimen in the plane of the loops. It is characteristic that in such an analysis only the derivative  $P_m \Delta z$  can be determined. At the same time the value of  $P_m$  is indeterminate and it is evidently limited by the value of  $P_m^{\text{ZFC}}$ , while  $\Delta z$  is appreciably less than the specimen diameter  $D$ , since the difference of this parameter from zero might be associated with the weak (by  $\alpha \leq 2-3^\circ$ ) departure from an angle of  $90^\circ$  between the plane of the film specimen and the  $z$  axis of the magnetometer (Fig. 6). If the value  $P_m^{\text{ZFC}}$  is used as  $P_m$  and  $\Delta z \approx D\alpha$  holds, then we can obtain  $\alpha = 1.7 \Delta P_m R / P_m^{\text{ZFC}} D \approx 14^\circ$  as a lower estimate of the parameter  $\alpha$ , which is larger than the possible error in the specimen orientation ( $\leq 1-2^\circ$ ). Therefore, the model of the mechanisms discussed in the present work cannot be the reason for the anomalous signal in the FC regime.

The real distribution of magnetic moments in the specimen is evidently more complicated than in such a simple model. In particular, a shift in the specimen relative to the magnetometer axis is possible. For example, if the moment  $P_m^+$  is parallel to the magnetometer axis while  $P_m^-$  is shifted by  $\Delta \rho$ , then the expression for the magnetometer signal can be obtained from Eqs. (1) and (2) by using the relation

$$|\mathbf{r} + \Delta \mathbf{r}|^{-3/2} \approx |\mathbf{r}|^{-3/2} \left[ 1 - \frac{3\mathbf{r} \cdot \Delta \mathbf{r}}{r^2} \right]. \quad (5)$$

As a result, the following expression can be obtained

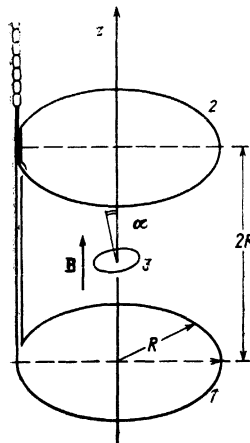


FIG. 6. Disposition of specimen 3 relative to pick-up coils 1 and 2 of the flux converter.

$$\Phi(z) = \Delta P_m \Phi(z) + \frac{3\mu_0 P_m R^2 \Delta \rho^2}{4} \times \left[ \frac{1}{[R^2 + (l/2 - z)^2]^{3/2}} - \frac{1}{[R^2 + (l/2 + z)^2]^{3/2}} \right]. \quad (6)$$

Qualitatively, however, this does not change the result, since the additional term also turns out to be odd with respect to  $z$ .

Another reason for an anomalous magnetometer response to arise could be the existence of a component of magnetization in a direction perpendicular to the external magnetic field. We are still not clear about the mechanism for such a component. Note that, e.g., the anisotropy signal of layered superconductors for an inclined orientation of the magnetic field leads to a pile-up of vortices in the basal plane of the specimen.<sup>16-20</sup> As is shown in Fig. 7, such a pile-up would lead to the appearance of a transverse component of magnetization, while the value of the longitudinal magnetization  $m^{\parallel} = (n - n_0)\Phi/\mu_0$  can turn out to be considerably less than the transverse  $m^{\perp} = n\Phi/\mu_0 (\sin \beta)$  ( $\beta$  is the angle of pile-up).

The appearance of a magnetic moment lying in the plane of the film cannot be associated with the Meissner signal in the plane of the film, since its magnitude calculated from the dimensions of the specimen, even for the case of the full Meissner effect, is appreciably less than the observed signal. Actually, for  $B = 40.74$  mT with the full Meissner effect, we have

$$P_{m\perp}^{full} \approx VB = \pi D^2 h B / 4 = 4 \cdot 10^{-8} \text{ A} \cdot \text{m}^2.$$

The real signal should be still smaller, since the film thickness is comparable with the penetration depth  $\lambda$ .

The existence of a magnetic moment  $P_m$  perpendicular to the external field and shifted by  $\Delta \rho$  relative to the axis leads to an additional signal being formed

$$\Delta \Phi(z) = \frac{3\mu_0 P_{m\perp} R^2 \Delta \rho \cos \alpha}{2} \times \left[ \frac{l/2 - z}{[R^2 + (l/2 - z)^2]^{3/2}} + \frac{l/2 + z}{[R^2 + (l/2 + z)^2]^{3/2}} \right], \quad (7)$$

where  $\alpha$  is the angle between the vectors  $P_m$  and  $\Delta \rho$ . This signal is asymmetrical in  $z$  and coincides with the second term of Eq. (4) to within a constant factor.

The dependence of the flux  $\Phi(z)$  through the pick-up coils of the flux converter can then be written in the form

$$\Phi(z) = \Phi_1(z) + \Phi_2(z),$$

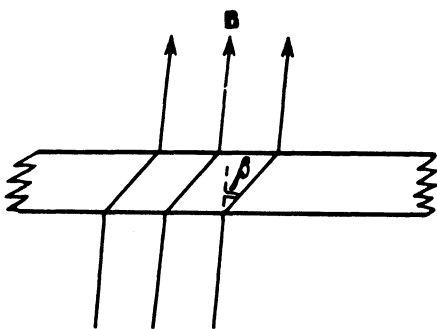


FIG. 7. Formation of a transverse moment on "pile-up" of vortices in the plane of the specimen.

where  $\Phi_1(z)$  is the response from a longitudinal film magnetization and  $\Phi_2(z)$  is the response from components lying in the plane of the loop. If the specimen is exactly on the  $z$  axis of the gradientometer, then the term  $\Phi_2(z)$ , according to Eq. (7), vanishes for any  $z$ . The shape of the signal  $\Phi(z)$  will be "correct" since it is only determined by  $\Phi_1(z)$ . However, a real specimen might be shifted by some distance  $\Delta \rho$  ( $\Delta \rho \ll R$ ) from the flux converter  $z$  axis. In this case the contribution from the horizontal component  $\Phi_2(z)$  cannot be neglected and the shape of the signal  $\Phi(z)$  will be determined by the superposition of the contributions  $\Phi_1$  and  $\Phi_2$ . As a result, the shape of the signal will be asymmetrical relative to the midpoint between the pick-up coils of the flux converter and numerically agrees satisfactorily with experiment. In particular, agreement with the experimental curve shown in Fig. 5a can be obtained for  $P_m \Delta \rho / \Delta P_m R \approx 1.7$ . If we set  $\Delta \rho \sim 1$  mm, then we can obtain for  $P_{m\perp}$  the value  $1.1 \times 10^{-5} \text{ A} \cdot \text{m}^2$ , which is considerably less than  $P_m^{full}$  and  $P_m^{ZFC}$ . It can arise for a small pile-up of vortices at an angle  $\beta = P_{m\perp} / P_m^{full} \approx 5$ .

Finally, the third possibility for the anomalous signal to arise could be nonuniformity in the external magnetic field. As can readily be understood from Fig. 8, a change in the magnitude of the external magnetic field by  $\Delta H$  when the specimen is moved between the pickup coils after cooling in the FC regime leads to the appearance of a signal  $\Delta P_m \approx \Delta P_m^{full}$ . Even for a small inhomogeneity in field it can exceed the value of  $P_m^{FC} = \chi^{FC} H$ , since  $\Delta P_m / P_m^{FC} \approx \Delta H / \chi^{FC} H$ . However, in our case the field is quite uniform,  $\Delta H / H \sim 10^{-3}$  (Fig. 9 and Ref. 3), and this mechanism should be unimportant. The  $\Phi(z)$  dependences studied are completely reversible, while for the mechanism in question the magnetometer response at the first shift should differ from the subsequent ones (see Figs. 8 and 9).

The importance of carefully fixing the external conditions is illustrated by the results of studying the angular dependence of the signal. As a consequence of the axial symmetry of the experimental set-up, as can readily be understood, there should be no angular dependence. However, as can be seen from Fig. 10, a fairly strong dependence was observed in the experiment. We assume that this result is associated with a small misorientation  $\Delta \alpha$  between the axis of rotation and the magnetic field, less than  $\Delta \alpha \leq 1^\circ$ . In this case the field precesses within a cone  $\Delta \alpha$  on rotating the specimen. As a result, the applied field along the specimen axis is modulated with an amplitude  $\geq H(\Delta \alpha)^2$ . To compensate these changes shielding currents arise which lead to amplitude modulation of the specimen's magnetic moment

$$\Delta P_m \geq H(\Delta \alpha)^2 V / (1 - N) = P_m^{full} (\Delta \alpha)^2 \approx 0.5 \cdot 10^{-7} \text{ A} \cdot \text{m}^2.$$

The analysis of the results obtained thus indicates that measurement of the magnetization of  $\text{YBa}_2\text{Cu}_3\text{O}_x$  films in the FC regime is a rather complicated problem for real experimental arrangements and requires high homogeneity and stability of the magnetic field. The magnetometer signal observed has an unusual character. It can be explained by the appearance of a transverse component in the magnetization of the specimen, and also the formation of an inhomogeneous magnetic state.

Such behavior may be characteristic for the FC regime

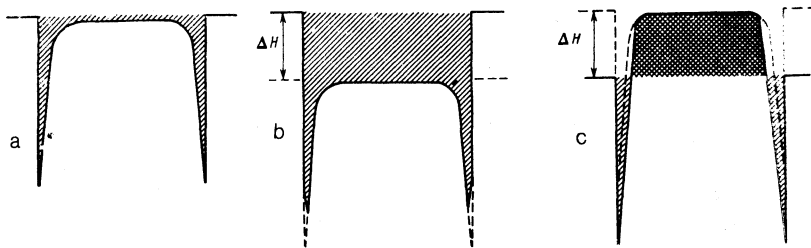


FIG. 8. Diagram of the distribution of magnetic induction within a specimen in the shape of an infinite plate, a) in the FC regime<sup>13</sup> and also on subsequent small b) increase and c) reduction in the applied field. The magnetic moment is determined by the difference between the areas with double and single hatching.

in high fields when the magnitude of the  $P_m^{\text{FC}}$  signal is very small. This, specifically, agrees with the work of Shcherbakov *et al.*<sup>21</sup> and Valiulin *et al.*,<sup>22</sup> where the appearance of a paramagnetic signal was observed in the FC regime for HT-SC single crystals and ceramics in strong magnetic fields  $> 2\text{--}3$  kOe, corresponding to  $\chi^{\text{FC}} < 10^{-3}$ .

### Critical currents

For a thin disk the relation between the critical current density  $j_c$  and the specific magnetization  $\delta P_m/V$  obtained in the Bean model<sup>9</sup> turns out to be just the same as for an infinite cylinder:

$$j_c = 3\delta P_m / VD, \quad (8)$$

where  $\delta P_m$  is the width of the hysteresis loop,  $D$  is the diameter, and  $V$  the volume of the specimen. The validity of this relation was verified experimentally by Oh *et al.*<sup>23</sup> and Obara *et al.*<sup>24</sup> by varying the dimensions of the film specimens.

On the basis of this expression critical current densities  $j_c$  were determined and their temperature and field dependences obtained using SQUID and vibration magnetometers, which differed greatly in the rate of change of magnetic field. In the first case it was  $dH/dt \sim 1$  kOe/h while in measurements with the vibration magnetometer it was  $dH/dt \sim 10^2$  kOe/h. As can be seen in Fig. 11, a small influence on  $j_c$  of the value of  $dH/dt$  is only observed at high temperatures.

It is not possible to express the temperature dependence  $j_c(T)$  for  $B \rightarrow 0$  over the whole temperature range either by an exponential  $j_c \propto \exp(-T/T_0)$  (Ref. 25) or by a linear  $j_c \propto (1 - T/T_0)$  (Refs. 26, 27) or by  $j_c \propto (1 - T/T_0)^\gamma$ , where  $\gamma \approx 1.5\text{--}2$  (Refs. 28, 29) dependence ( $T$  is a constant). However, as for  $\text{YBa}_2\text{Cu}_3\text{O}_x$  single crystals,<sup>30</sup> the temperature dependence of  $j_c$  can be described by an empirical relation

$$j_c(T) = j_{c0} [\exp(-T/T_0) - \exp(-T_c/T_0)]. \quad (9)$$

At high temperatures (Fig. 11a range 50–80 K) it gives a linear  $j_c$  dependence and at low temperatures an exponen-

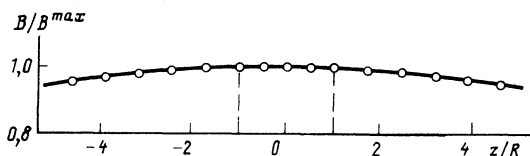


FIG. 9. Distribution of magnetic field induction (longitudinal component) along the magnetometer  $z$  axis;  $R$  is the radius of the pick-up loops of the flux converter (dashed lines).

tial. Curves corresponding to Eq. (9) for values of the parameters  $j_{c0} = 1.8 \times 10^7$  A/cm<sup>2</sup>,  $T_c = 90.5$  K and  $T_0 = 350$  K are shown by the full lines in Fig. 11. It should be noted that the value of  $T_0$  for  $\text{YBa}_2\text{Cu}_3\text{O}_x$  films, like  $j_{c0}$ , is an order of magnitude greater than the corresponding values for single crystals ( $T \sim 10$  K,  $j_c \sim 10^6$  A/cm<sup>2</sup>, for example, Ref. 31). We also note that although Eq. (9) is empirical, it represents fairly well the temperature dependence  $j_c(T)$  over the whole temperature range below  $T_0$  not only for  $\text{YBa}_2\text{Cu}_3\text{O}_x$  films, but also for single crystals of  $\text{YBa}_2\text{Cu}_3\text{O}_x$  (Ref. 30), monodomain  $\text{TmBa}_2\text{Cu}_3\text{O}_x$  crystals<sup>31</sup> and single crystals of the organic superconductor  $\kappa\text{-(BEDT-TTF)}_2\text{Cu(NCS)}$  and evidently appears to be fairly universal.

The field dependence  $j_c(B)$  cannot be represented over the whole magnetic field range satisfactorily by any simple relation. As is seen from Fig. 12, in the weak field region  $B < 200\text{--}300$  mT, an exponential field dependence works satisfactorily:

$$j_c(B, T) = j_c(0, T) \exp(-B/B_0) \quad (10)$$

( $B_0$  is a constant). However, at higher fields appreciable departures from it are observed. A better agreement for higher fields is observed with the classic dependence (Fig. 13):

$$j_c(B, T) = j_c(0, T) \frac{B_0(T)}{B_0(T) + B}. \quad (11)$$

We also note that the rate at which the magnetic field  $B$  is applied and the magnitude of the characteristic measuring

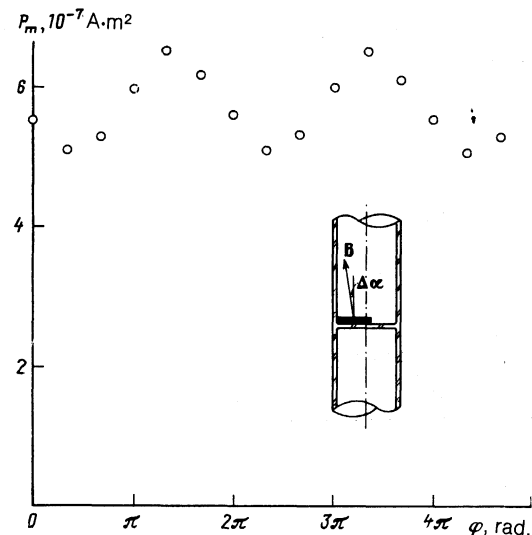


FIG. 10. Angular dependence of the  $P_m^{\text{FC}}$  signal for a disk of  $\text{YBa}_2\text{Cu}_3\text{O}_x$  film after FC in a field  $B = 34.08$  mT,  $T = 4.2$  K,  $B \parallel c$ .

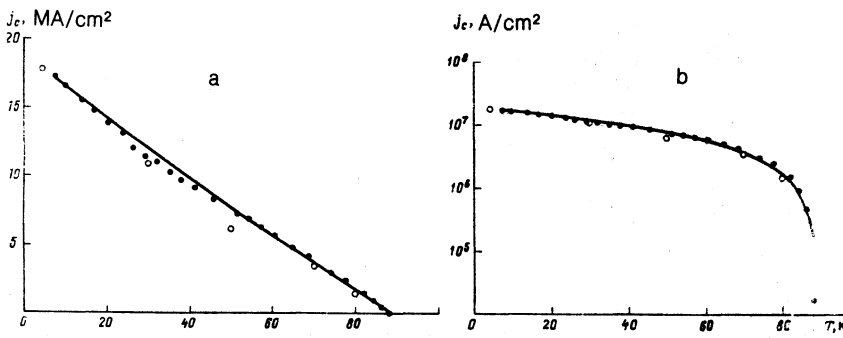


FIG. 11. Temperature dependence of the critical current density  $j_c$  ( $B = 0$ ) on a) linear and b) logarithmic scales. Experimental results obtained with (●) vibration and (○) SQUID magnetometers. The full line corresponds to calculation based on Eq. (9) with  $j_{c0} = 1.8 \times 10^7$  A/cm<sup>2</sup>,  $T_c = 90.5$  K and  $T_0 = 350$  K.

time of the apparatus  $\tau^*$  have an appreciable influence on the form of  $j_c(B)$  because of strong magnetic moment relaxation processes, which are especially significant at high temperatures.

There is a universal behavior of the magnetization curves if  $B_0(T)/j_c(0, T) = \text{const}$ . This follows from the fact that the magnetic moment of a disk in the critical state is determined by the expression

$$P_m(H_e) = \frac{1}{2} \int [j_c \mathbf{r}] dV = \pi j_c(0, T) \int [\mathbf{e}_\varphi \mathbf{r}] f\left(\frac{B(H_e, \mathbf{r})}{B_0}\right) dV, \quad (12)$$

where  $H_e$  is the strength of the external field,  $f(B)$  is a function expressing the field dependence of  $j_c$  and  $\mathbf{e}_\varphi$  is the basis vector of the cylindrical coordinate system. According to the Biot-Savart-Laplace law, the value of the magnetic induction is determined by the expression

$$B(H_e, \rho, z) = \mu_0 H_e + \frac{\mu_0}{4\pi} \int \frac{[j_c(\mathbf{r}-\mathbf{r}')]}{|\mathbf{r}-\mathbf{r}'|^3} dV' = \mu_0 H_e + \frac{\mu_0 j_c(0, T)}{2} \int \frac{[\mathbf{e}_\varphi(\mathbf{r}-\mathbf{r}')]}{|\mathbf{r}-\mathbf{r}'|^3} f\left(\frac{B(H_e, \mathbf{r}')}{B_0}\right) dV'. \quad (13)$$

Then

$$\frac{P_m(B, T)}{P_m(0, T)} = \left| \int [\mathbf{e}_\varphi \mathbf{r}] f\left(\frac{B(H_e, \mathbf{r})}{B_0}\right) dV \right| / \left| \int [\mathbf{e}_\varphi \mathbf{r}] f\left(\frac{B(0, \mathbf{r})}{B_0}\right) dV \right|, \quad (14)$$

$$\frac{P_m(0, T)}{B_0} = \frac{\pi j_c(0, T)}{B_0} \left| \int [\mathbf{e}_\varphi \mathbf{r}] f\left(\frac{B(0, \mathbf{r})}{B_0}\right) dV \right|,$$

$$\frac{B(H_e, \mathbf{r})}{B_0(T)} = \left| \frac{\mu_0 H_e}{B_0(T)} + \frac{\mu_0 j_c(T, 0)}{2B_0(T)} \times \int \frac{[\mathbf{e}_\varphi(\mathbf{r}-\mathbf{r}')]}{|\mathbf{r}-\mathbf{r}'|^3} f\left(\frac{B(H_e, \mathbf{r}')}{B_0}\right) dV \right| = \psi\left(\frac{\mu_0 H_e}{B_0(T)}, \frac{j_c(T, 0)}{B_0(T)}\right),$$

where  $\psi$ , as above, is some scaling function. It follows from this that for  $B_0(T)/j_c(0, T) = \text{const}$ .

$$\frac{P_m(B)}{P_m(0)} = \psi\left(\frac{H_e}{P_m(0)}\right). \quad (15)$$

It can be seen from Fig. 14 that the requirement  $B_0(T)/j_c(0, T) = \text{const}$  is satisfied over a wide temperature range  $T = 20-80$  K. It is just in this temperature region that the scaling of the magnetization curves is observed (see Fig. 3), which is an experimental demonstration of Eq. (15). Near  $T_c$  the departure from it is evidently associated with the transition from creep to viscous flux flow, while at low temperatures the departure can be explained by the incomplete penetration of magnetic flux to the center of the specimen.

The existence of a difference between  $j_c$  determined from magnetic measurements ( $j_c^m$ ) and from current-voltage characteristics ( $j_c^i$ ) has been pointed out in the literature.<sup>32</sup> Agreement between  $j_c^m$  and  $j_c^i$  is only observed in the weak field region.<sup>33-35</sup> It was thus interesting to compare the value of the critical current density  $j_c^d$  obtained for a specimen in the form of a disk from the half-width  $\Delta P_m$  of the hysteresis loop according to the Bean model<sup>9,36</sup>  $j_c^d = 3\Delta P_m/RV$  for specimens in the shape of a disk and thin

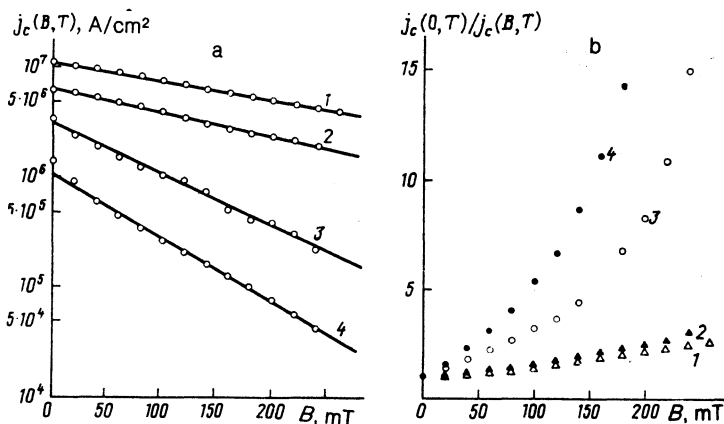


FIG. 12. Field dependence of a) direct and b) inverse critical current density of  $\text{YBa}_2\text{Cu}_3\text{O}_x$  films,  $B \parallel c$  for different temperatures: 1) 30 K; 2) 50 K; 3) 70 K; 4) 80 K. The experimental results were obtained from measurements using the SQUID magnetometer.

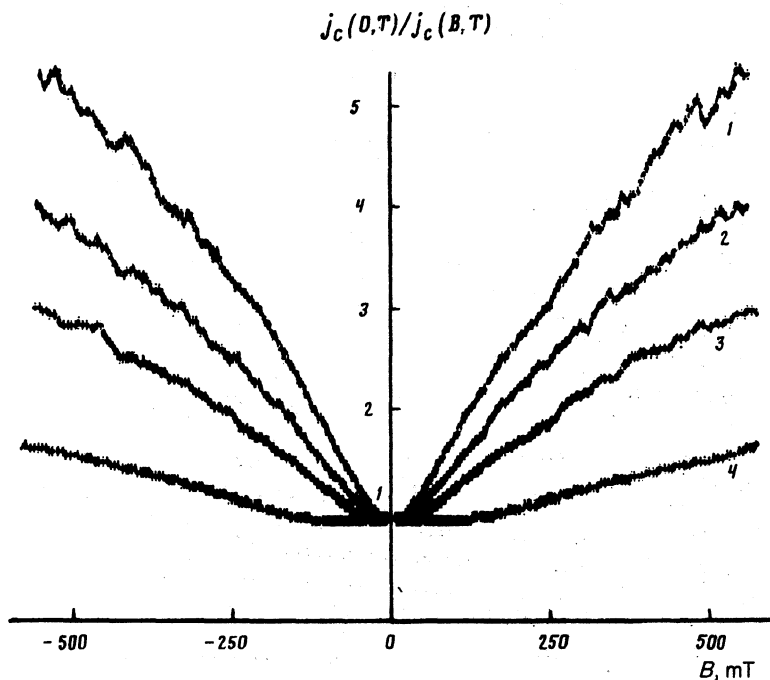


FIG. 13. Field dependence of inverse critical current density of a  $\text{YBa}_2\text{Cu}_3\text{O}_x$  film,  $\mathbf{B} \parallel \mathbf{c}$ , for different temperatures: 1) 69 K; 2) 54 K; 3) 32 K; 4) 7.3 K. The experimental results were obtained using the vibration magnetometer.

ring, prepared from one and the same film, with the value of  $j'_c$  in a thin ring for which the magnetic moment  $P'_m$  is determined by the relation  $P'_m = j'_c S S_{cr}$ , where  $S$  is the area of the ring,  $S_{cr}$  is the cross section, and  $P'_m$  is the maximum magnetic moment when magnetic reversal occurs.

The critical current densities obtained in this way agree satisfactorily with one another:

$$j'_c = 4.0 \cdot 10^9 \text{ A/cm}^2 \approx 3.5 \cdot 10^9 \text{ A/cm}^2 = j_c^d \text{ for } B \rightarrow 0, T = 70 \text{ K.}$$

However, the field dependences  $j_c(B)$  for ring and disk differ considerably (Fig. 15). This dependence is weaker for a ring, while the value of  $B_0$  (Fig. 16) is appreciably higher. The results on the critical current of a ring  $j'_c$  are thus closer to results obtained from current-voltage measurements  $j'_c$ .

This behavior can evidently be explained by magnetic flux creep.<sup>32</sup> As a result of this process the magnitude of the measured critical current depends on the threshold voltage  $E_c$  (Ref. 37):

$$j_c = j_{c0} \left[ 1 - \frac{kT}{U} \ln \frac{E_0}{E_c} \right], \quad (16)$$

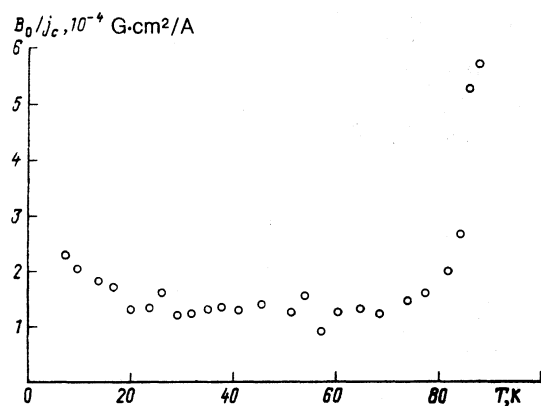


FIG. 14. Temperature dependence of  $B_0(T)/j_c(0,T)$  for a  $\text{YBa}_2\text{Cu}_3\text{O}_x$  film,  $\mathbf{B} \parallel \mathbf{c}$ . The parameters  $B_0(T)$  and  $j_c(0,T)$  correspond to Eq. (11) and were obtained from measurements with the vibration magnetometer.

here  $U$  is the activation energy,  $E_0 = B\nu_0 d$ , where  $\nu_0$  is a characteristic frequency and  $d$  is the characteristic jump distance. For  $B = 100 \text{ mT}$ ,  $\nu_0 = 10^{12} \text{ Hz}$  and  $d = 10 \text{ nm}$ <sup>38</sup> the value of  $E_0$  is  $\sim 10^3 \text{ V/m}$ . The value of  $E_c$  for a ring is determined by the Faraday law:

$$E_c = \frac{1}{2\pi R} \pi R^2 \frac{dB}{dt} = \frac{R}{2} \frac{dB}{dt}. \quad (17)$$

If the experimental parameters  $dB/dt = 10 \text{ T/h}$  and  $R \approx 1 \text{ mm}$  are used, then we can obtain  $E_c \sim 10^{-6} \text{ V/m}$ , which is appreciably less than typical values  $\geq 10^{-4} \text{ V/m}$  used for resistive measurements. It is difficult to determine the value of  $E_c$  for a disk, but it is seen from Eq. (17) that it should be less. The influence of creep effects should thus decrease as we go over successively from disk to ring and to the resistive measuring method. In addition, as a result of the increase in  $E_0$  the influence of these effects should grow with the magnetic field.

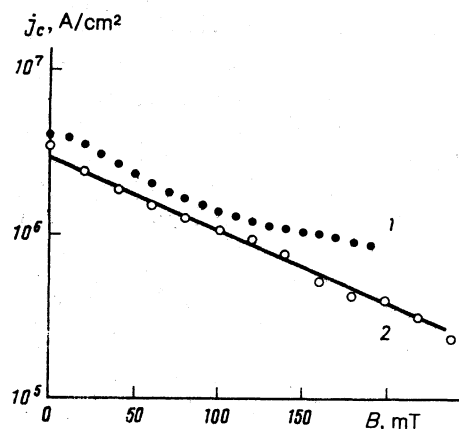


FIG. 15. Field dependence of critical current density for  $\text{YBa}_2\text{Cu}_3\text{O}_x$  film specimens in the shape of 1) a disk and 2) a ring at  $T = 70 \text{ K}$ ,  $\mathbf{B} \parallel \mathbf{c}$ .

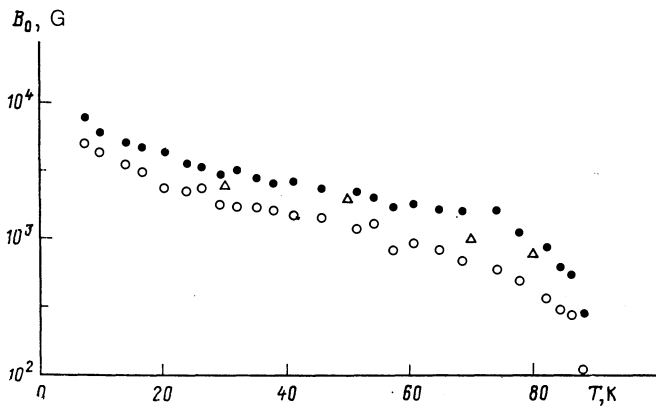


FIG. 16. Temperature dependence of the parameter  $B_0$ . The experimental results were obtained on the basis of measurements with ( $\Delta$ ) the SQUID and ( $\circ, \bullet$ ) the vibration magnetometers and correspond to ( $\Delta, \bullet$ ) Eq. (10) and ( $\circ$ ) Eq. 11.

### Relaxation time of the magnetization

The logarithmic relaxation  $R = dP_m/d(\ln T)$  of the magnetization of HTSCs first observed by Müller *et al.*<sup>39</sup> and Klimenko and Kim,<sup>40</sup> has been well studied in HT-SC films (see, for example, Refs. 28, 29, 41, 42). However, while the temperature dependence of the rate of logarithmic relaxation  $R(T)$  of the magnetization of thin films has been studied fairly fully,<sup>43,44</sup> the behavior of the  $R(B)$  dependence has so far not been studied. In the present work the relaxation of magnetization in different magnetic fields and at different temperatures has been investigated.

The time dependence of the magnetic moment in a

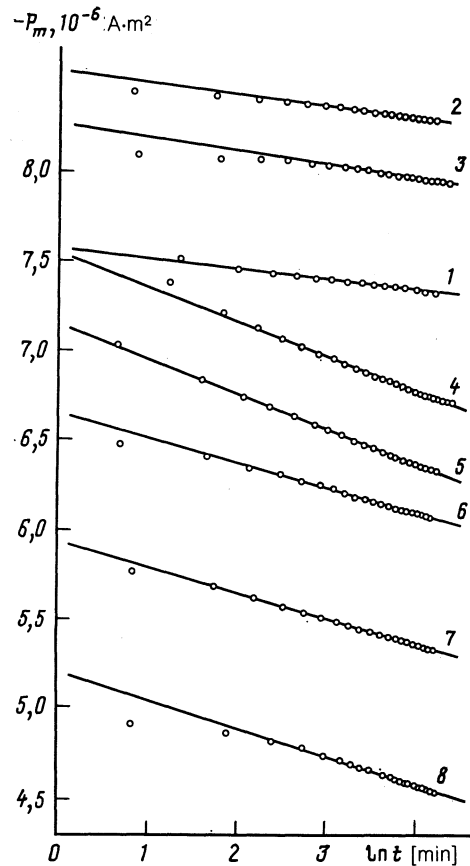


FIG. 17. Dependence of the magnetic moment of a disk of  $\text{YBa}_2\text{Cu}_3\text{O}_x$  film on  $\ln t$ ,  $T = 70 \text{ K}$ ,  $\mathbf{B} \parallel \mathbf{c}$ , for different values of  $B$  (in mT): 1) 8.46; 2) 11.894; 3) 13.88; 4) 18.36; 5) 26.27; 6) 34.72; 7) 43.00; 8) 51.95.

$\text{YBa}_2\text{Cu}_3\text{O}_x$  disk  $P_m^{\text{ZFC}}$ , in different magnetic fields after ZFC up to 70 K is shown in Fig. 17. It is seen that the relation  $P_m \propto \ln(t/\tau_0)$  describes the experimental results well, starting from some characteristic time  $\tau_0 > 10^2 \text{ s}$  after the application of magnetic field  $B$ . The departure from logarithmic relaxation at times less than  $t_0$  has been noted earlier.<sup>45-48</sup> For classical type-II superconductors the time  $t_0$  is an order of magnitude less (see, for example, Alekseevskii *et al.*<sup>49</sup> and Mitin<sup>50</sup>). The nonlogarithmic character of relaxation at small times is evidently due to viscous flux flow for  $j > j_c$ .<sup>9,51</sup>

The  $P_m(\ln t)$  dependence was used to investigate  $R(B)$  in two regimes: ZFC to  $T_0$  and application of the field ( $P_m^{\text{ZFC}}$ ) and FC to  $T_0$ , and removal of the field accompanied by the appearance of a remanent magnetization (RM) relaxing with time ( $P_m^{\text{RM}}$ ).

The specimen was inserted in the upper loop of the flux converter of the SQUID magnetometer and fixed there for a detailed investigation of the initial nonlogarithmic segment of the time dependence  $P_m(t)$ . The change with time in the magnetic flux through the pick-up coil of the flux converter of the magnetometer due to the change in magnetic moment of a disk of  $\text{YBa}_2\text{Cu}_3\text{O}_x$  film was measured after the application of field  $B$ . The time dependence  $P_m(t)$  could be obtained, starting  $t^* \approx 3 \text{ s}$  after application of the field  $B$ , which is two orders of magnitude less than the time of the first measurement with the standard procedure of measuring magnetization (see, for example, Yeshurin *et al.*<sup>52,53</sup> and McHenry *et al.*<sup>54</sup>)

The time dependence  $P_m(\ln t)$  at  $T = 50 \text{ K}$  and  $B = 54 \text{ mT}$  in two regimes (ZFC and RM) is shown in Fig. 18. They are characterized by some difference in the relaxation rates  $R$ . The ratio of logarithmic relaxation rates is

$$\frac{R^{\text{RM}}}{R^{\text{ZFC}}} = \frac{dP_m^{\text{RM}}/d(\ln t)}{dP_m^{\text{ZFC}}/d(\ln t)} \approx 1.1.$$

It can be shown that within the framework of the Bean model the relaxation rate in the critical state is described by the expression<sup>9</sup>

$$R = \frac{kT}{U_0} \frac{j_c D}{3}, \quad (18)$$

where  $U_0$  is the mean activation energy. The main difference between the ZFC and FC regimes is that in the first case an external field is applied to the specimen while in the second it is absent and the specimen is in the field provided by internal

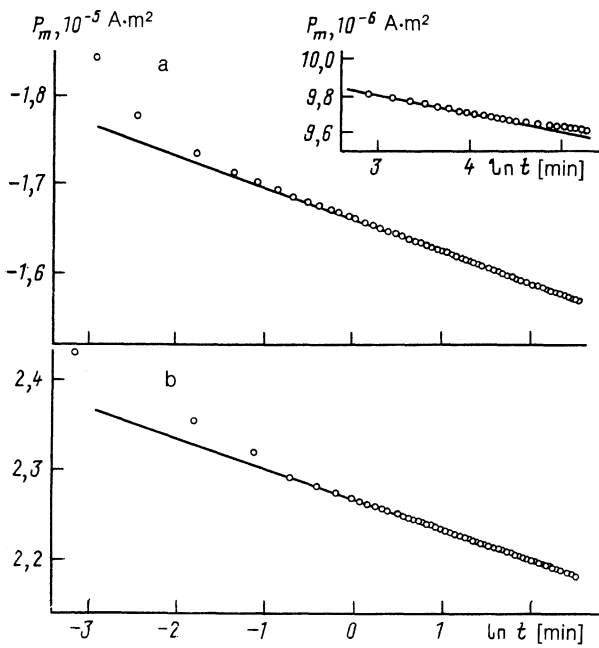


FIG. 18. Initial sections of the dependence of magnetic moment of a disk of  $\text{YBa}_2\text{Cu}_3\text{O}_x$  film on  $\ln t$ ,  $T = 50$  K,  $\mathbf{B} \parallel \mathbf{c}$ : a) ZFC and application of field  $B$ ; b) FC and removal of  $B$ . The inset shows the section of the dependence for large times at  $T = 70$  K,  $\mathbf{B} \parallel \mathbf{c}$ .

currents which in general are appreciably smaller in magnitude. Consequently, according to Eq. (18) the ratio of relaxation rates should be determined by the critical currents:

$$\begin{aligned} R^{\text{ZFC}}/R^{\text{FC}} &= j_c(54 \text{ mT})/j_c(0 \text{ mT}) \\ &\approx 6,3 \cdot 10^6 \text{ A/cm}^2 : 5,25 \cdot 10^6 \text{ A/cm}^2 \approx 1,2, \end{aligned}$$

which agrees satisfactorily with the experimental value.

For larger times ( $t \approx 3$  h), as can be seen from the inset to Fig. 18, a departure from the  $P_m(\ln t)$  relation is observed. This agrees with earlier results<sup>55</sup> and corresponds to the theoretical model<sup>56</sup> which predicts a transition from a logarithmic to an exponential relaxation for long times.

The field dependence of the rate of logarithmic relaxation  $R^{\text{ZFC}}$  at  $T = 70$  K,  $\mathbf{B} \parallel \mathbf{c}$  is shown in Fig. 19; this has a maximum at  $B \approx 20$  mT, associated with a topological transition in the distribution of shielding Bean currents.<sup>9,51</sup> For a disk of diameter  $D$  and thickness  $h$  the field for the topological transition  $H_t$  is satisfactorily described by the relation<sup>9,51</sup>

$$H_t - H_{c1} = \frac{j_c(T, B)h}{2} \ln \left[ \frac{D + (D^2 + h^2)^{1/2}}{h} \right] \quad (19)$$

taking into account that  $H_{c2} \rightarrow 0$  for  $T = 70$  K and  $j_c \approx 35 \times 10^6 \text{ A/cm}^2$ .

In order to exclude the influence of  $j_c(B)$  on the rate of logarithmic relaxation  $R$ , the reduced relaxation rate,<sup>9</sup> shown in Fig. 19b is introduced:

$$S(B) = \frac{R}{\Delta P_m} = \frac{1}{\Delta P_m} \frac{dP}{d(\ln t)} = \frac{kT}{U_0} \quad (20)$$

In a field  $B \gg B_t \approx 20$  mT, corresponding to the complete penetration of shielding currents to the center of the specimen, the  $S(B)$  dependence reaches a constant value equal to

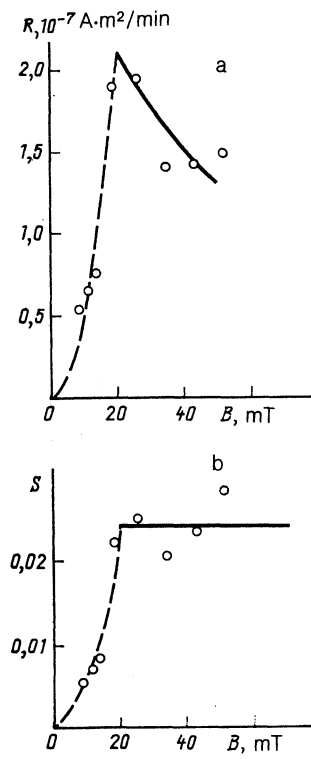


FIG. 19. Field dependence of the (a) rate of logarithmic relaxation  $R$  and (b) reduced relaxation rate  $S$  of the magnetic moment of a disk of  $\text{YBa}_2\text{Cu}_3\text{O}_x$  film,  $T = 70$  K,  $\mathbf{B} \parallel \mathbf{c}$ .

$kT/U_0$ , from which the magnitude of the characteristic pinning energy  $U_0 \approx 0.25$  eV can be determined, and this agrees in order of magnitude with the value of  $U_0$  determined for  $\text{YBa}_2\text{Cu}_3\text{O}_x$  (Refs. 32, 33) and  $\text{TlBaCaCuO}$  (Refs. 7, 8) films.

As the temperature decreases the value of  $j_c$  increases, which in agreement with Eq. (19) should lead to an increase in the field  $H_t$ . The shift in the maximum of  $R(B)$  actually corresponds to a change in critical current density  $j_c$ . The ratio calculated on the basis of Eq. (19)

$$\begin{aligned} H_t(T=4,2 \text{ K})/H_t(T=70 \text{ K}) \\ = j_c[H_t(T=4,2 \text{ K})]/j_c[H_t(T=70 \text{ K})] \approx 5,2 \end{aligned}$$

agrees with the value found experimentally,  $H(T_t = 4.2 \text{ K})/H(T_t = 70 \text{ K}) \approx 4$  (Fig. 20).

## CONCLUSIONS

1. The magnetization curves  $P_m(B)$  of epitaxial  $\text{YBa}_2\text{Cu}_3\text{O}_x$  films have been investigated. Over a wide temperature range  $20 \text{ K} < T < 80 \text{ K}$  the  $P_m(B)$  dependences have similar shape and obey the scaling law

$$P_m(B, T) = P_0(T) \varphi_s [B/\mu_0 P_0(T)],$$

where  $\varphi_s$  is the scaling function.

2. An anomalous state forms for  $T < T_c$  in the FC regime. It is shown that its appearance can be associated with three causes: the formation of an inhomogeneous state, inhomogeneity in the magnetic field, and pile-up of vortices in the plane of the specimen. From a numerical analysis the last is the most likely.

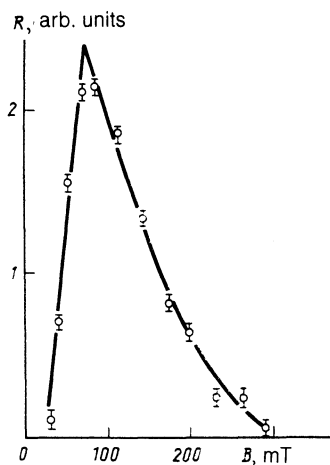


FIG. 20. Field dependence of the relaxation rate of the magnetic moment of a disk of  $\text{YBa}_2\text{Cu}_3\text{O}_x$  film,  $T = 4.2$  K,  $B \parallel c$ .

3. The temperature and field dependence of the critical current density calculated from the magnetization curves have been studied. It was established that the temperature dependence is described well by a linear dependence on  $T$  at high temperatures and an exponential at low temperatures, or by the empirical relation

$$j_c(T) = j_{c0} [\exp(-T/T_0) - \exp(-T_c/T_0)]$$

over the whole range below  $T_c$ . The field dependence in the low field region ( $\leq 0.3$  T) can be represented in the form

$$j_c(B, T) = j_c(0, T) \exp(-B/B_0).$$

Satisfactory agreement in the case of large fields is obtained with the relation

$$j_c(B, T) = j_c(0, T) \frac{B_0(T)}{B_0(T) + B}.$$

4. The field dependence of thermally activated creep of magnetic flux has been studied. The existence was established of a maximum in the rate of logarithmic relaxation, which is associated with a topological transition in the distribution of the shielding Bean currents. This relaxation rate increases up to the point of the topological transition  $B_t$  and then reaches a constant value which enables the mean activation energy  $U_0$  of the Abrikosov vortices to be determined in the specimens studied. Its value of 0.25 eV is considerably greater than the corresponding value for single-crystals, which corresponds to the higher values of  $j_c$  in films.

<sup>1</sup> D. I. Mendeleev Chemicotechnical Institute, Moscow

<sup>2</sup> P. N. Lebedev Physics Institute, Academy of Sciences of the USSR

<sup>1</sup> K. K. Likharev, V. K. Semenov, and A. B. Zorin, *Results on Science and Technology*, VINITI, Moscow (1988).

<sup>2</sup> E. V. Pechen', A. V. Varlashkin, A. I. Golovashkin *et al.*, *Physical Chemistry and Technology of Superconducting Materials* [in Russian], Nauka, Moscow (1988).

<sup>3</sup> V. D. Kuznetsov, *Prib. Tekh. Eksp.* No. 4, 196 (1985).

<sup>4</sup> M. Tinkham, *Rev. Mod. Phys.* **36**, 268 (1964).

<sup>5</sup> A. A. Ginnius, V. V. Moshchalkov, S. A. Pozigin, M. V. Semenov, V. I. Voronkova, and V. K. Yanovskii, *Fiz. Tverd. Tela (Leningrad)* **30**, 3485 (1983) [*Sov. Phys. Solid State* **30**, 2002 (1983)].

<sup>6</sup> R. B. van Dover, L. F. Schneemeyer, E. M. Gyorgy, and J. V. Waszczak, *J. Appl. Phys.* **52**, 1910 (1988).

<sup>7</sup> S. Hatta, Y. Ichikawa, H. Adachi, and K. Wasa, *Jpn. J. Appl. Phys.* **28**, L794 (1989).

<sup>8</sup> S. Hatta, Y. Ichikawa, H. Adachi, and K. Wasa, *Jpn. J. Appl. Phys.* **28**, L422 (1989).

<sup>9</sup> V. V. Moshchalkov, A. A. Zhukov, L. I. Leonyuk *et al.*, *Superconductivity: Physics, Chemistry, Technology*, **2**, No. 12, 84 (1989).

<sup>10</sup> Y. Wulfus, Y. Yeshurun, I. Felner, and H. Sompolinsky, *Phys. Rev.* **B40**, 2701 (1989).

<sup>11</sup> M. Cerdonio, C. Cosmelli, G. L. Romani, C. Messina, and G. Gramaccioni, *Rev. Sci. Instrum.* **47**, 1 (1976).

<sup>12</sup> V. D. Kuznetsov, *Izv. Vyssh. Ucheb. Zaved. Fiz.* No. 2, 40 (1984).

<sup>13</sup> A. A. Zhukov, V. V. Moshchalkov, V. D. Kuznetsov *et al.*, *Superconductivity: Physics, Chemistry, Technology*, **3**, 603 (1990).

<sup>14</sup> L. Ya. Vinnikov, I. V. Grigor'eva, L. Ya. Gurevich, and A. E. Koshelev, *Superconductivity: Physics, Chemistry, Technology*, **3**, 50 (1990).

<sup>15</sup> P. Leiderer, P. Brüll, T. Klumpp, and B. Stritzker, *Physica (Utrecht)* **B165-166**, 1387 (1990).

<sup>16</sup> N. Alekseyevsky, *J. Phys. USSR* **10**, 360 (1946).

<sup>17</sup> M. Däumling and D. C. Larbalestier, *Phys. Rev.* **B40**, 9350 (1989).

<sup>18</sup> A. I. Buzdin and A. Yu. Simonov, *Pis'ma Zh. Eksp. Teor. Fiz.* **51**, 168 (1989) [*JETP Lett.* **51**, 191 (1989)].

<sup>19</sup> D. E. Farrell, C. M. Williams, S. A. Wolf, N. P. Bansal, and V. G. Kogan, *Phys. Rev. Lett.* **61**, 2805 (1988).

<sup>20</sup> V. G. Kogan, *Phys. Rev.* **B24**, 1572 (1981).

<sup>21</sup> A. S. Shcherbakov, V. F. Startsev, E. G. Valiulin, and A. N. Petrov, *J. Phys.: Condens. Matter* **2**, 2199 (1990).

<sup>22</sup> E. G. Valiulin, A. A. Druzhinin, V. E. Startsev, and A. S. Shcherbakov, *Pis'ma Zh. Eksp. Teor. Fiz.* **49**, 664 (1989) [*JETP Lett.* **49**, 763 (1989)].

<sup>23</sup> B. Oh, M. Naito, S. Arnason, P. Rosenthal, R. Barton, M. R. Beasley, T. H. Geballe, R. H. Hammond, and A. Kapitulnik, *Appl. Phys. Lett.* **51**, 852 (1987).

<sup>24</sup> H. Obara, S. Kosaka, M. Umeda, and Y. Kimura, *Physica (Utrecht)* **B165-166**, 1413 (1990).

<sup>25</sup> T. Fukami, T. Kamura, A. A. A. Youssef, Y. Horie, and S. Mase, *Physica (Utrecht)* **C159**, 427 (1989).

<sup>26</sup> K. Setsune, Y. Ichikawa, T. Kamada, K. Hirochi, H. Adachi, S. Kohiki, and K. Wasa, *Cryogenics* **29**, 296 (1989).

<sup>27</sup> A. Mogro-Campero, L. G. Turner, and E. L. Hall, *J. Appl. Phys.* **65**, 4951 (1989).

<sup>28</sup> J. W. C. de Vries, M. A. M. Gijs, G. M. Stollman, T. S. Baller, and G. N. A. van Veen, *J. Appl. Phys.* **64**, 426 (1988).

<sup>29</sup> S. V. Gaponov, F. V. Garin, V. N. Golubev, V. F. Garin, M. A. Kolyagin, E. B. Klyuenkov, V. Y. Kosyev, A. V. Kochemasov, and M. D. Strikovskii, *Zh. Eksp. Teor. Fiz.* **95**, 1086 (1989) [*Sov. Phys. JETP* **68**, 625 (1989)].

<sup>30</sup> I. V. Gladyshev, S. N. Gordeev, *et al.* *Physica (Utrecht)* **B165-166**, 1631 (1990).

<sup>31</sup> V. V. Moshchalkov, A. A. Zhukov, D. K. Petrov, V. I. Voronkova, and V. K. Yanovskii, *Physica (Utrecht)* **C166**, 185 (1990).

<sup>32</sup> P. Fischer, H.-W. Neumüller, B. Roas, H. F. Braun, and G. Saemann-Ischenko, *Solid State Commun.* **72**, 871 (1989).

<sup>33</sup> G. M. Stollman, B. Dam, J. H. P. M. Emmen, and J. Pankert, *Physica (Utrecht)* **C159**, 854 (1989).

<sup>34</sup> L. Z. Avdreev, A. V. Volkozub, A. I. Golovashkin, E. V. Ekimov, S. I. Krasnovobodsev, K. K. Likharev, E. V. Pechen', O. V. Snigirev, and V. V. Khanin, *Pis'ma Zh. Eksp. Teor. Fiz.* **47**, 508 (1988) [*JETP Lett.* **47**, 594 (1988)].

<sup>35</sup> A. Schuhl, R. Cabanel, S. Koch, J. Siejka, M. Touzeau, J. P. Hirtz, and G. Creuzet, *Physica (Utrecht)* **C162-164**, 627 (1989).

<sup>36</sup> C. P. Bean, *Rev. Mod. Phys.* **36**, 31 (1964).

<sup>37</sup> A. M. Campbell and J. E. Evetts, *Adv. Phys.* **21**, 199 (1972).

<sup>38</sup> T. T. M. Palstra, B. Batlogg, R. B. van Dover, L. F. Schneemeyer, and J. V. Waszczak, *Phys. Rev.* **B41**, 6621 (1990).

<sup>39</sup> K. A. Müller, M. Takashige, and J. G. Bednorz, *Phys. Rev. Lett.* **58**, 1143 (1987).

<sup>40</sup> A. G. Klimenko and V. A. Kim, *Problems in High-Temperature Superconductivity* [in Russian], Inst. Metal Phys., Sverdlovsk (1987).

<sup>41</sup> J. Lensink, C. F. J. Flipse, J. Roobeek, R. Griessen, and B. Dam, *Physica (Utrecht)* **C 162-164**, 663 (1989).

<sup>42</sup> N. Kobayashi, H. Kawabe, H. Iwasaki, K. Watanabe, H. Yamane, H. Kurosawa, H. Masumoto, T. Hirai, T. Matsushita, and Y. Muto, *Physica C162-164*, 683 (1989).

<sup>43</sup> E. L. Venturini, J. F. Kwak, D. S. Ginley, R. J. Baughman, and B. Morosin, *Physica C162-164*, 673 (1989).

<sup>44</sup> M. Nakao, K. Kawaguchi, H. Furakawa, K. Shikichi, and Y. Matsuta, *Physica C162-164*, 677 (1989).

<sup>45</sup> N. E. Alekseevskii, A. V. Mitin, E. P. Khlybov, G. M. Kuz'micheva, V. I. Nizhankovskii, J. Warchulska, and A. Gilewski, *Zh. Eksp. Teor. Fiz.*

- 97, 263 (1990) [Sov. Phys. JETP 70, 148 (1990)].
- <sup>46</sup> M. Földeaki, M. E. McHenry, and R. C. O'Handley, Phys. Rev. **B39**, 11475 (1989).
- <sup>47</sup> C. Rossel, Y. Maeno, and I. Morgenstern, Phys. Rev. Lett. **62**, 681 (1989).
- <sup>48</sup> C. Rossel, Y. Maeno, and F. H. Holtzberg, IBM J. Res. Dev. **33**, 328 (1989).
- <sup>49</sup> N. E. Alekseevskii, A. V. Mitin, and E. P. Khlybov, Zh. Eksp. Teor. Fiz. **82**, 927 (1982) [Sov. Phys. JETP **55**, 543 (1982)].
- <sup>50</sup> A. V. Mitin, Zh. Eksp. Teor. Fiz. **93**, 590 (1987) [Sov. Phys. JETP **66**, 335 (1987)].
- <sup>51</sup> V. V. Moshchalkov, A. A. Zhukov, V. D. Kuznetsov, V. V. Metlushko, and L. I. Leonyuk, Pis'ma Zh. Eksp. Teor. Fiz. **50**, 81 (1989) [JETP Lett. **50**, 91 (1989)].
- <sup>52</sup> Y. Yeshurun, A. P. Malozemoff, T. K. Worthington, R. M. Yandrofski, L. Krusin-Elbaum, F. H. Holtzberg, T. R. Dinger, and G. V. Chandrasekhar, Cryogenics **29**, 258 (1989).
- <sup>53</sup> Y. Yeshurun, A. P. Malozemoff, F. H. Holtzberg, and T. R. Dinger, Phys. Rev. **B38**, 11828 (1988).
- <sup>54</sup> M. E. McHenry, M. P. Maley, G. J. Kwey, and J. D. Thompson, Phys. Rev. **B39**, 7339 (1989).
- <sup>55</sup> A. C. Mota, A. Pollini, P. Visani, and G. Juri, Physica (Utrecht) **C162-164**, 695 (1989).
- <sup>56</sup> C. W. Hagen, R. P. Griessen, and E. Salomons, Physica (Utrecht) **C157**, 199 (1989).

Translated by R. Berman